Biomaterials and Biosystems 6 (2022) 100050

Contents lists available at ScienceDirect

Biomaterials and Biosystems

journal homepage: www.elsevier.com/locate/bbiosy

Application of bioengineered elastin-like polypeptide-based system for targeted gene delivery in tumor cells☆

Aena Yi[1], Dahye Sim[1], Seon-Boon Lee, Vijaya Sarangthem*, Rang-Woon Park*

Department of Biochemistry and Cell Biology, Cell & Matrix Research Institute, School of Medicine, Kyungpook National University, Daegu, 41944, Republic of Korea

ARTICLE INFO

Keywords:
AP1-ELPs
IL-4 receptor
ELP
Cell-penetrating peptide
EGFP expression
Gene delivery

ABSTRACT

Successful gene delivery depends on the entry of negatively charged DNAs and oligonucleotides across the various barriers of the tumor cells and localization into the nucleus for its transcription and protein translation. Here, we have reported a thermal responsive self-assemble and highly biocompatible, targeted ELP-based gene delivery system. These systems consist of cell-penetrating peptides, Tat and single or multiple repeats of IL-4 receptor targeting peptide AP-1 along the backbone of ELP. Cell-penetrating peptides were introduced for nuclear localization of genes of interest, AP-1 for targeting IL-4R highly expressed tumor cells and ELP for stable condensation favoring protection of nucleic acids. The designed multidomain fusion ELPs referred to as Tat-ELP, Tat-A_1E_{28} and Tat-A_4V_{48} were employed to generate formulation with pEGFP-N1. Profound formulation of stable complexes occurred at different molar ratios owing to electrostatic interactions of positively charged amino acids in polymers with negatively charged nucleic acids. Among the complexes, Tat-A_4V_{48} containing four copies of AP-1 showed maximum complexation with pEGFP-N1 in lower molar ratio. The polymer-pEGFP complexes were further analyzed for its transfection efficiency in different cancer cell lines. Both the targeted polymers, Tat-A_4V_{48} and Tat-A_1E_{28} upon transfection displayed significant EGFP-expression with low toxicity in different cancer cells. Therefore, both Tat-A_4V_{48} and Tat-A_1E_{28} can be considered as novel transfection system for successful gene delivery with therapeutic applications.

1. Introduction

At present, various gene transfer systems have been developed with the intent to produce great extents of therapeutic proteins for the treatment of various diseases, including cancer, genetic disorders, and infectious diseases [1–4]. The wide range of non-viral delivery systems were investigated from past decades to achieve several parameters, such as the protection of genetic materials, bypassing of several membrane barriers, high transfection efficiency with minimal toxicity [5,6]. The polymers for example polyethyleneimine (PEI), and carbon nanotubes, PEG (polyethylene glycol), PLL (poly-L-lysine), chitosan and PLGA (polylactic-coglycolic acid) etc. are widely used gene delivery systems [7–11]. But complexity of controlling the molecular weight and polydispersity increase the risk of possible toxicity [12]. Thus, an approach of using recombinant peptides was being employed for high potency transfer of genetic materials with less toxicity. Cell-penetrating peptides (CPPs) are commonly used short peptides for gene delivery because of their ability to condense DNA efficiently into compact nanoformulations through electrostatic interactions [13,14]. Among various CPPs, penetratin (Pen) peptide from Antennapedia [15], the Tat peptide from the HIV-1 Tat protein [16] and Bac peptide from the bovine antimicrobial bactenecin peptide Bac 7 etc. [17] are commonly used for membrane translocation. TAT peptide has useful attributes for cancer therapy as it makes the conjugated molecule internalize the cell more efficiently, followed by the ability to target specific compartments. Additionally, it was observed that the TAT contains a nuclear localization signal that significantly enhances transfection efficiency. Despite having useful attributes in gene delivery, CPP need to overcome the collateral cytotoxicity effect due to lack of specificity [18–20]. Thus, the strategy of conjugating an overexpressed surface molecule or receptor-specific peptide ligands to the CPPs will permit targeting to those receptors in a cell-specific manner and have been proven to be a safer substitute. It was reported that chimeric multidomain fusion protein, consisting of ErbB-2 receptor binding single chain antibody fused with the exotoxin translocation domain of Pseudomonas and a DNA-binding domain was able to transfect ErbB-2-expressing tumor cells in vitro in a cell's specific manner [21].

In this context, a novel recombinant elastin-like polypeptides (ELPs) based system has useful characteristics and advantages over existing polymer carriers for gene delivery [22–24]. ELPs are a stimulus-

☆ This paper was authored by the EiC of the journal, but the editorial process of the paper was handled by Manuel Salmeron-Sanchez.

* Corresponding authors.
E-mail addresses: devi1703@gmail.com (V. Sarangthem), nwpark@knu.ac.kr (R.-W. Park).

[1] Aena Yi and Dahye Sim equally contributed to this work

https://doi.org/10.1016/j.bbiosy.2022.100050
Received 25 December 2021; Received in revised form 28 March 2022; Accepted 15 April 2022

responsive biopolymer derived from the hydrophobic domain of human tropoelastin therefore ideal for gene delivery as they are less likely to be toxic [25]. It consists of pentapeptide repeats such as Val–Pro–Gly–Xaa–Gly (VPGXG), where X represents a guest residue that can be any amino acid except proline (Pro) [26]. The genetic-engineering methods for synthesis of ELP allow absolute control over the architecture, including physical or chemical properties, especially surface charge, polydispersity, aggregation, and biocompatibility at the gene level [27]. These unique properties allow multipurpose use of ELP in different fields like drug delivery, regenerative medicine, and tissue engineering etc [28–32]. They exhibit reversible phase transitions from soluble to insoluble aggregates at a certain temperature, known as transition temperature (Tt). ELPs are soluble in aqueous solutions below their transition temperatures (Tt) but insoluble above. This phase transition is highly dependent on the guest residue, ionic state, and molecular weight [33]. Consecutively, ELPs can be easily incorporated with biofunctional groups or crosslinking peptides either at the polypeptide termini or flanked by pentapeptide repeats of ELPs without compromising with their thermally responsive behavior [34,35]. Even by varying the amino acid composition or including positively charged residues in ELP molecules, the stability under physiological conditions can be improved. The fusion of ELPs with cell-penetrating peptides (CPP) has been employed as a promising vector for delivering drugs and therapeutic peptides into solid tumors [36,37]. Recently, it was reported that the fusion of oligolysine along ELPs significantly encapsulated plasmid DNA and delivered into the cells. However, although effective DNA delivery, cytotoxicity effects due to the oligolysine residues were observed [38].

As ELP can be precisely designed at the molecular level through recombinant DNA engineering, here we are attempting to develop an ELP-based targeted carrier to overcome limitations of other polymers and improve the delivery of genetic materials. Exploiting the facile recombinant technique, Tat (a CPP) peptide and single or multiple copies of AP-1 (an IL-4 receptor specific ligand) was incorporated into an ELP molecule to facilitate their ability to condense DNA for gene delivery. AP-1 is an atherosclerotic plaque and breast tumor tissue-homing peptide, which was discovered by the phage screening method [39,40]. It specifically targets interleukin-4 receptors (IL-4Rs), which are highly expressed in a wide variety of human solid tumors, including renal cell carcinoma, squamous cell carcinoma of the head and neck, malignant glioma, AIDS-associated Kaposi's sarcoma, and breast carcinoma [41–44].

Recently, we have described the potency of Tat and AP1 functionalized ELPs constitutes (Tat-A1E_{28} or Tat-A_4V_{48}) in delivering siRNA to the target site of action and inducing significant gene silencing activity in murine breast carcinoma 4T1 allograft mice model [45]. In this study, functionalized ELPs were further analyzed for its role in delivering DNA, as an approach for effective therapy against cancer, autoimmune and infectious disease etc. Herein, the tumor-specific delivery of plasmids bearing EGFP genes by functionalized ELPs was studied in different cancer cell lines. The transfection mechanisms mediated by ELPs-DNA complexes, including cellular uptake, payload release and expression of genes of interest in vitro were well investigated.

2. Materials and methods

2.1. Cell culture

Human breast carcinoma cell MDA-MB231, canine epithelial kidney cell MDCK, human lung cancer cell lines H460 and A549 cells were obtained from the American Type Culture Collection (ATCC). MDA-MB231 and MDCK cells were grown in Dulbecco's modified Eagle's medium (DMEM) (Hyclone, Invitrogen, Carlsbad, CA, USA) containing 10% fetal bovine serum (Gibco, Canada) and 100 U/mL penicillin and 100 μg/mL streptomycin (Sigma Aldrich). Human lung cancer cell lines, A549 and H460 were maintained in RPMI-1640 medium (Gibco, Canada). Cells were maintained at 37°C in a humidified 5% CO_2 atmosphere.

2.2. Nomenclature

We used ELP variants (E_{28}, Tat-E_{28}, Tat-A_1E_{28}, and Tat-A_4V_{48}) for DNA delivery applications. Here, E_{28} stands for [$V_8F_2G_3A$-2], where the guest residue X of ELP pentapeptide VPGXG was substituted with Valine, Phenylalanine, Glycine and Alanine. A_1 and A_4 of Tat-A_1E_{28}, and Tat-A_4V_{48} specified one or four unit of targeting peptide AP-1. In Tat-A_4V_{48}, V_{48} represents 48 monomers of VPGVG pentapeptides.

2.3. Thermal characterization

All polypeptides (E_{28}, Tat-E_{28}, Tat-A_1E_{28} and Tat-A_4V_{48}) were diluted to 25 and 50 μM with phosphate saline-buffered (PBS) and their transition temperatures (Tt) were determined by monitoring turbidity profiles at 350 nm between the temperature range of 20°C and 55°C using UV-visible spectrophotometer. The absorbance was monitored while increasing temperature at 1°C/min.

The phase transition of respective polypeptides after complexation with nucleic acid was further analyzed. To determine the Tt of ELPs/pEGFP-N1 complexes, 1 μg of pEGFP-N1 plasmid was mixed with respective ELP variants (25-200 μM) at a molar ratio of 1:25 to 1:200 (DNA: ELPs). Tt values were determined at 350 nm from 20°C to 55°C using a UV-visible spectrophotometer.

2.4. Gel retardation assay

To assess the ability of complexation of respective polypeptides with DNA, a gel retardation assay was performed. pEGFP (1μg) of plasmid DNA was mixed with various concentrations of ELPs (25-200 μM) and incubated for 20 min at room temperature to form ELPs/pEGFP complexes with different molar ratios (mixtures were adjusted with DEPC water to the same volume). Samples were prepared by mixing DNA and ELPs at a constant molar ratio and subjected to 1% agarose gel electrophoresis in the TBE buffer to confirm encapsulation.

2.5. DNase A stability test

DNase I digestion test was performed to assess the ability of ELPs in preventing pEGFP from nuclease degradation [46]. ELPs/pEGFP complexes was prepared by mixing 500 ng of pEGFP with 200 μM of ELP variant (i.e., E_{28}, Tat-E_{28}, Tat-A_1E_{28} or Tat-A_4V_{48}) and treated with 1.5 μl of EDTA (50 mM) to terminate the reaction. DNase I activity was then inactivated at 65 °C for 15 min. Afterward, for dissociation of complexes 6 μl of heparin sodium (2 μl/ml) (JW Pharmaceutical, S. Korea) were added to each protein mixtures and subsequently incubated at 37 °C for 2 h. Later, the reaction mixture was subsequently analyzed on 1% agarose gel electrophoresis in TBE buffer system.

2.6. Determination of particle sizes and surface charges

All ELPs were diluted to 25 μM with phosphate saline-buffered (PBS) and particle size distributions and zeta potentials was determined using an ELS-Z2 (Otsuka Electronics Korea Co, Ltd., Korea). ELPs/pEGFP complex were also prepared using PBS in the same manner at a molar ratio of 1:200 (pEGFP-N1: ELPs). Particle size distributions and surface charges of complexes were further examined using the ELS-Z2. The shapes and sizes of nanocomplexes were further examined by transmission electron microscopy (TEM, CM30 Electron Microscope, Philips, CA). ELPs/pEGFP complexes were dropped on the grid and allowed to dry for 10 min and after negative staining with 2 wt.% uranyl acetate solution was observed using the TEM.

2.7. Analysis of transfection efficiencies by pEGFP/ELPs

ELPs/pEGFP complexes were prepared at a molar ratio of 1:200. Briefly, 1 μg of pEGFP was mixed with 200 μM of each ELP variant in

Opti-MEM reduced serum medium. MDA MB231 (2.5×10^5) cells grown to 80% confluence in 6-well plates were treated with ELPs/pEGFP complexes for 6 h and media were then replaced with complete media. EGFP expression levels in transfected cells were also visualized by fluorescence microscopy 48 h after transfection.

The correlation of transfection efficiency in relation with level of IL-4R expression was examined using different cell lines such as MDA MB231, H460, and A549, including normal epithelial kidney cell lines MDCK. Briefly, 10^5 cells each type were plated in 24 well-plates and incubated with the ELP/pEGFP complexes for 4 h. Then, media were replaced with complete media and incubated for 48 h. To observe the transfection efficiency, the cells were collected after trypsinization and centrifuged at 1500 rpm for 3 min. After washing with PBS, the cells were resuspended in 0.3 ml PBS and transfection efficiency was measured using BD FACS Aria system (Becton–Dickinson, USA).

Additionally, the transfection efficiency was assessed in the presence and absence of serum. MDA-MB231 and A549 cells were treated with complexes for 4 h in complete media containing 10% FBS or 10% FBS with 5% glycerol. The cells were trypsinized 48 h following transfection, and the expression of EGFP was analysed by FACS.

2.8. Cytotoxicity assay

5×10^3 of MDA MB231 and A549 cells per well were individually seeded in 96-well plates and cultured for 24 h to achieve 75–85% confluence. Then, cells were incubated with 0.2 ml of fresh serum containing DMEM containing various ELP/pEGFP complexes for 4 h. The cells were re-cultured in fresh complete media. After 48 h post incubation, 10 μl of CCK-8 stock solution (Dojindo Molecular Technology Inc.) was added to each well. Optical density was measured at 450 nm using an ELISA microplate reader (Bio-Rad, USA) after 1 h of incubation. The relative cytotoxicity was calculated as a percentage of absorbance of the treated to untreated cells.

2.9. Statistical analysis

The significance of differences between the test and control groups were analyzed using the student's t-test for two groups or by one-way analysis of variance (ANOVA) for more groups. Statistical significance was set for p values of $^{***}P < 0.0001$ and is denoted by asterisks in all figures.

3. Results

3.1. Preparation of the ELP variant and its physical characterization

In this study, we focused on the investigation of ELP variants (E_{28}, Tat-E_{28}, Tat-A_1E_{28}, and Tat-A_4V_{48}) in terms of physical and biochemical properties for enhanced DNA delivery applications. The ELP variants were precisely constructed using recombinant DNA engineering by combining the coding sequence of Tat (cell-penetrating peptide, CPP) and IL-4 receptor specific-targeting ligand (AP1) along with ELP sequence and synthesized as monodisperse molecules in bacterial cultures (Fig. 1A). Two ELP variants, Tat-A_1E_{28} (A_1 represent one AP1-unit and E_{28} represent 28 ELP repeat and Tat-A_4V_{48} (A_4 represent four AP1-unit and V_{48} represent 48 repeats of ELP) were used as tumor-specific vectors. On the other hand, Tat-E_{28} and E_{28} were used as non-targeted vectors. It was already depicted that the positively charged Arginine, (R) residue present in Tat (YGRKKRRQRRR) and AP-1 (RKRLDRN) in ELP variants facilitated siRNA condensation, causing nano-complex formation. Similarly, positive-charged arginine (R) residue in ELP variants would easily bind with DNA molecules in order to form a stable nano-formulation (Fig. 1A). With these multidomain ELP variants, it is anticipated there will be an enhanced transfection efficiency in IL-4R highly expressing tumor cells, with more nuclei-localized genetic materials for better expression of targeted genes (Fig. 1B). All the ELPs were successfully expressed in Escherichia coli and purified by exploiting the inverse phase cycling method. Thus, after four cycles of repeated heating and cooling followed by centrifugation, resulted in high purities. Protein purity and molecular weights were confirmed by SDS-PAGE followed by copper chloride (0.3 M) staining (Fig. S1). A SDS-PAGE showed that the molecular weights were nearly equivalent to the theoretical MW calculation using amino acid contents as follows; E_{28} (12.18 KDa), Tat-E_{28} (13.19 KDa), Tat-A_1E_{28} (15.00 KDa), and Tat-A_4V_{48} (26.81 KDa).

3.2. Gel retardation and stability assay

ELPs are further investigated for their ability to interact with DNA molecules, which is vital for successful transfection. At first complexes of DNA and ELPs were prepared by mixing 1 μg of pEGFP-N1 with different concentrations of ELPs (25-200 μM), incubated at room temperature for 20 min and mobilities were assessed using an agarose gel DNA mobility assay. The ELP variants such as Tat-E_{28}, Tat-A_1E_{28} and Tat-A_4V_{48} showed effective condensation with DNA, indicated by retarded migration of pEGFP-N1 at different molar ratios. The association of pEGFP-N1with ELP variants was evident at molar ratios of 200:1(200 μM of ELPs: 1 μg pEGFP). Among ELPs, Tat-A_4V_{48} showed efficient encapsulation of pEGFP-N1 at a lower molar ratio of 50:1 (Tat-A_4V_{48}: pEGFP). Whereas Tat-A_1E_{28} achieved complete complexation with pEGFP-N1 at molar ratios of 150:1 (Tat-A_1E_{28}: pEGFP) and Tat-E_{28} at 200:1 (Tat-E_{28}: pEGFP), respectively (Fig. 1C). The control E_{28} did not encapsulate plasmid DNA at any concentration showing Tat and AP1 were solely responsible for the observed interactions.

Next, the stability of ELPs/pEGFP complexes against DNase I degradation was investigated by incubating the complexes with or without DNase I for 3 h at 37 °C. A DNase I protection test aimed at evaluating the stability of ELPs/pEGFP complexes was done at 200:1 molar ratio. As indicated in Fig. 1D, naked pEGFP and sample containing E_{28}/pEGFP was completely digested by DNase I (lane 3 and lane 5, respectively). While Tat-E_{28}/pEGFP, Tat-A_1E_{28}/pEGFP and Tat-A_4E_{48}/pEGFP, (lane 7, lane 9 and lane 11) DNA bands remained in the lane, suggesting the ability to protect DNA from DNase I degradation.

3.3. Biophysical characterization of ELPs/pEGFP complexes

The sizes, and surface charges of ELPs/pEGFP complexes in comparison with naked ELPs were characterized through DLS. Parallel measurements of particle sizes of complexes revealed dramatic increases in particle sizes when Tat-E_{28}, Tat-A_1E_{28} and Tat-A_4V_{48} was condensed with pEGFP. The sizes of E_{28}, Tat-E_{28}, Tat-A_1E_{28}, and Tat-A_4V_{48} were 390, 78.1, 30.1 and 29 nm respectively. After complex formation, the average particle diameters of Tat-E_{28}, Tat-A_1E_{28} and Tat-A_4V_{48}/pEGFP complexes raised upto 182.8 ± 21.1 nm, 234.9 ± 14.3 and 578.3 ± 18.8 nm, respectively (Table 1). Since E_{28} protein did not interact with pEGFP, no changes in sizes or charges were observed. In addition, surface charges of ELPs/pEGFP complexes were analyzed using the zeta potential analyzer. The condensation of ELPs with pEGFP resulted in a slight decrease in the zeta potential compared with naked ELPs (Table 1). The sizes and structure of nanocomplex after association with pEGFP were further confirmed by transmission electron microscopy (TEM). The TEM images of Tat-A_1E_{28} and Tat-A_4V_{48} complexes displayed dispersed spherical nanostructures (Fig. 1E), while no particle formation was detected in the case of E_{28} complexes.

The thermal behaviors of the ELPs were monitored by measuring turbidity profiles using UV-visible spectrophotometry at 350 nm (OD_{350}) while increasing temperature at 1°C/min. The transition temperature, T_t values (defined as the temperature at which turbidity of a protein solution reached 50%) were determined at a concentration of 25 μM (Fig. 2A-D) and 50 μM (Fig. S2A-2D) in PBS. The Tt values of E_{28}, Tat-E_{28}, Tat-A_1E_{28} and Tat-A_4V_{48} were ~37°C, 40.5°C, 42.3 and 36.7°C, respectively. Further analysis of turbidity profile after complexation with

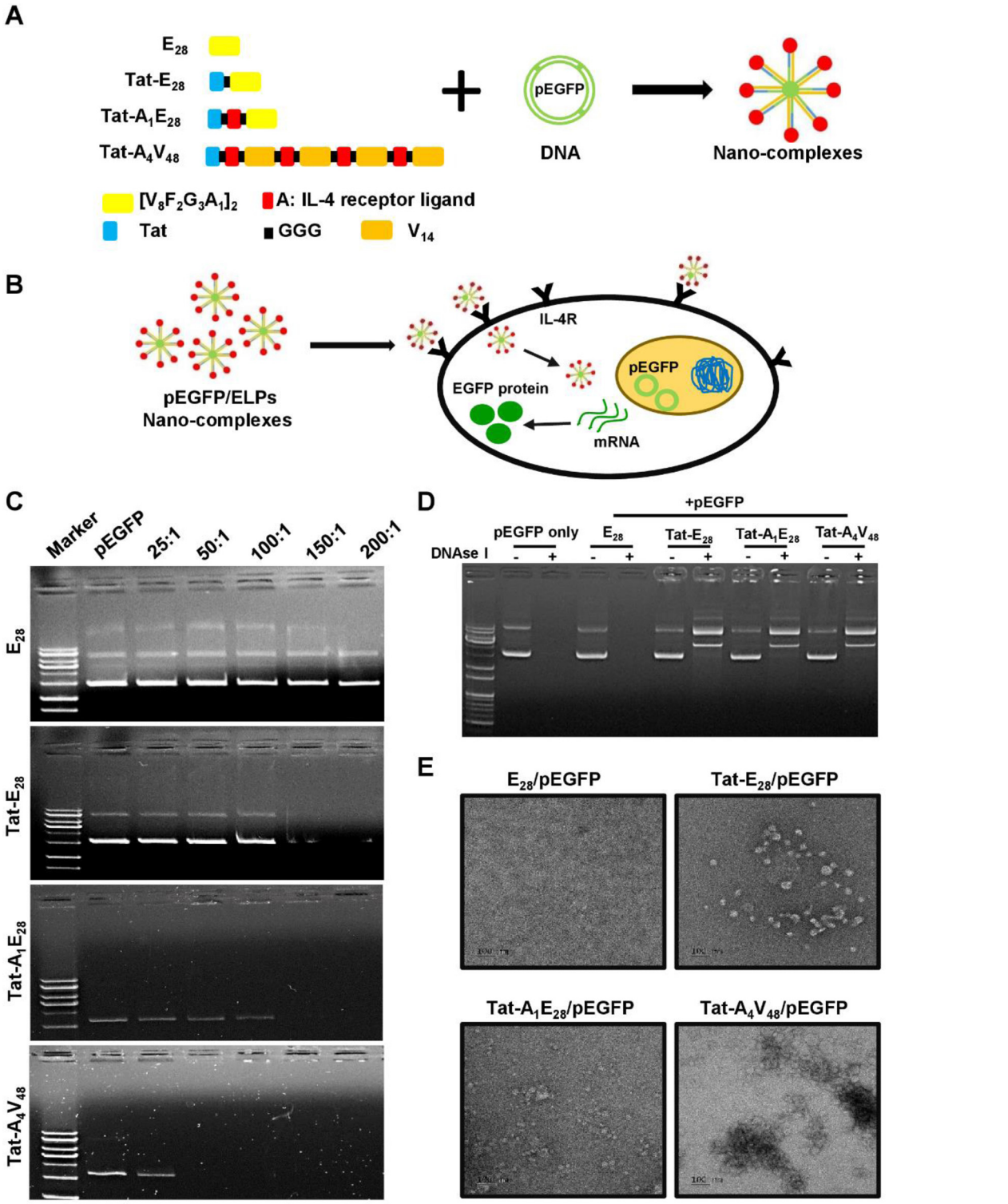

Fig. 1. ELPs/pEGFP formulation and mechanism of trasfection (A) Schematic representation of the amino acid sequences of the ELP variants (E_{28}, Tat-E_{28}, Tat-A_1E_{28}, and Tat-A_4V_{48}). The positively charged Arginine (R) residue present in ELPs induced complexation with negatively charged DNA to form nano-complex. (B) Targeted-ELPs variants allowed efficient transfection to IL-4R highly expressing tumor cells, bypass the nuclear membrane, successfully delivered the DNA molecules where it was transcribed, then translated the gene of interest. (C) Interactions between pEGFP (1 μg) and the ELPs (E_{28}, Tat-E_{28}, Tat-A_1E_{28}, and Tat-A_4V_{48}) were assessed using a gel retardation assay at various ELPs to pEGFP molar ratios (25 to 200 μM :1μg). Gels were visualized by staining with ethidium bromide. Lane 1: 1 kb DNA ladder, naked plasmid DNA. Lane 2: naked pEGFP (4733 bp), Lanes 3–5: ELPs/pEGFP complexes at different molar ratios. (D) Stability of ELPs/pEGFP complexes were determined through DNase I protection assay, complexes were prepared by mixing 1 μg of pEGFP with 200 μM of ELPs in the presence or absence of DNase I. The naked pEGFP (lanes 2 and 3) is loaded with or without DNase I. The lanes 4-11 indicate complexes treated or untreated with DNase I. (E) TEM images of ELPs/pEGFP complexes at room temperature. Scale bar, 100 nm.

Table 1
Physical characteristics of ELP variants before and after the encapsulations of pEGFP.

	Free ELPs			ELPs/pEGFP-N1complex		
ELPs	Tt (°C)[1]	Diameter (nm)[2]	Zeta-potential (mV)[3]	Tt (°C)[1]	Diameter (nm)[2]	Zeta-potential (mV)[3]
E_{28}	36.8	390.6± 57.2	1.90± 1.2	36.8	390.6± 57.1	1.91±1.2
Tat-E_{28}	40.5	78.1± 29.9	2.68±1.8	40.5	182.8 ± 21.1	-2.1±0.1
Tat-A_1E_{28}	42.3	30.1± 2.7	5.82±2.8	42.6	234.9 ± 14.3	4.3±0.8
Tat-A_4V_{48}	36.7	29± 7.1	0.097±0.6	36.47	578.3 ± 18.8	0.68±0.2

ELPs signifies E_{28}, Tat-E_{28}, Tat-A_1E_{28} and Tat-A_4V_{48}.[1]Transition temperatures (Tt) implies 50% of maximum coacervation of ELPs in aqueous solution. [2] Mean diameters of ELP variants as determined by dynamic light scattering analysis.[3]Zeta-potentials of ELPs and ELPs/pEGFP complexes. Errors designate ±SD from at least three separate experimentations.

pEGFP revealed no significant changes in the transition temperature upon complex formation.

3.4. The ELPs/pEGFP complexes mediated transfection in MDA MB231

In vitro transfection experiments were executed to determine the suitability of the ELPs/pEGFP complexes for application in gene delivery. Confocal images taken at 48 h after transfection confirmed the enhanced green fluorescence (EGFP) expression in MDA MB231 cells. Profound EGFP expression was observed in cells transfected with Tat-A_4V_{48}/pEGFP followed by relatively lesser EGFP expression in Tat-E_{28}/pEGFP transfected cells (Fig. 2E), and no EGFP expression was observed in E_{28}/pEGFP transfected cells.

3.5. Determination of transfection efficiency of ELPs/pEGFP in different cancer cells

Having visualized the transient transfection potential of ELPs/pEGFP complexes in MDA MB231, we further quantified the selective transfection activity in different cell lines. Tumor cells line H460, (Fig. 3C, D), MDA MB231 (Fig. 3E, F) and A549 (Fig. 3G, 3H) along with normal kidney cells MDCK (Fig 3A, B) were treated with E_{28}, Tat-E_{28}, Tat-A_1E_{28}, or Tat-A_4V_{48}/pEGFP complexes and subjected to flow cytometry 48 h post-transfection. MDA MB231 and A549 cells were used to determine the targeting ability of Tat-A_1E_{28}, or Tat-A_4V_{48} toward IL-4R (IL-4R positive) compared to MDCK and H460 cells with low IL-4R expression. All the complexes displayed minimum or no transfection in terms of enhanced green fluorescence expression in MDCK and H460 cells. In MDA MB231, the percentage of enhanced green fluorescence expression was observed to be 73.01 and 69.30% in cells transfected with Tat-A_1E_{28} or Tat-A_4V_{48}/pEGFP, respectively (Fig. 3F). Non–targeted Tat-E_{28} displayed 48.6 % EGFP gene expression, whereas no expression was observed in E_{28} mediated transfection.

Comparatively, Lipofectamine 2000 showed lower transfection efficiency in MDA MB231 or H460 and higher in MDCK (48.93%) or A549 (36.36%). These results clearly indicated that Tat-A_1E_{28}, or Tat-A_4V_{48} possess greater transfection efficiency and cell selectivity than the controls and Lipofectamine 2000. Furthermore, the time-dependent analysis, after complex treatment for 1, 3, and 6 h revealed a subsequent increase of EGFP expression as a function of time (Fig. S3A-S3C).

Likewise, Tat-A_1E_{28} or Tat-A_4V_{48}/pEGFP demonstrated 25.5 and 77.1 % enhanced green fluorescence expression in A549 cells (Fig. 3H). Tat-E_{28} or E_{28} mediated transfection showed 9.6% and 0.3% enhanced green fluorescence expression. Thus, higher transfection efficiency induced by Tat-A_1E_{28} or Tat-A_4V_{48}/pEGFP complexes in both MDA MB231 and A549 cells clearly indicated dependency of IL-4R expression. The fact that only IL-4R highly expressing cells were well transfected specified that the complexes were internalized by IL-4R mediated endocytosis.

3.6. Effect of ELPs/pEGFP complexes on transfection under different conditions and cytotoxicity assay

To further study the potential of ELPs in vitro gene delivery, ELPs/pEGFP complexes at their optimal molar ratios (1:200) were incubated with MDA MB231 and A549 cells under serum conditions. As shown in Fig. 4A and C, the transfection efficiency of Tat-A_4V_{48}/pEGFP in both cells were reduced under serum (10%) conditions. But incubation in the presence of 5% glycerol with serum further enhanced transfection efficiencies in both the cell lines (Fig. 4B and Fig. 4D). Targeting multidomain polymer, Tat-A4V48 could retain and even have higher transfection activity under serum-containing media after stabilizing of complexes with glycerol. No significant changes in the EGFP expression were observed in MDCK cells transfected with Tat-A_1E_{28} or Tat-A_4V_{48}/ pEGFP complexes under serum conditions (Fig. S5).

The cytotoxicity of ELPs/pEGFP complexes prepared at 1:200 molar ratio was also evaluated in the absence/presence of serum in MDA MB231 (Fig. 4E) and A549 (Fig. 4F) cells. ELPs/pEGFP complexes transfected cell lines showed above 80% cell viability, suggesting the safety of the complexes for gene transfection. There was a slight decrease in the percentage of cell viability in MDA MB231 cells, treated with Tat-A_4V_{48}/pEGFP complexes in the absence of serum. But under serum condition the viability of the transfected cells was almost like that of untreated control. Overall, the incubation of cells with ELPs/pEGFP complexes did not affect cell viability and they are very less toxic to the cells.

4. Discussion

Designing of multidomain peptides consisting of CPP along with targeting ligands are commonly exploited for formulations with genetic materials to facilitate the specific gene delivery. Using this approach, DNA will be easily interacted with, followed by enhanced uptake due to receptor-mediated endocytosis. In this study, we have reported a novel multifunctional thermal responsive, targeted ELP-based gene delivery system consisting of Tat and single or multiple repeats of IL-4 receptor targeting peptide AP-1 along the backbone of ELP. Through recombinant DNA engineering, ELP variants were precisely constructed to have useful attributes in gene delivery and purified with ease using E. coli bacterial system [45]. The phase transition characteristic of ELPs allows for separation by simple, inexpensive, batch non-chromatographic method called Inverse Transition Cycling (ITC).

Our investigations on the condensations of pEGFP with Tat-E_{28}, Tat-A_1E_{28} and Tat-A_4V_{48} revealed successful encapsulation at different molar ratios. Among the ELP variants, targeted polymers (Tat-A_1E_{28} or Tat-A_4V_{48}) could condense DNA more effectively, could easily be associated with the cellular membranes and subsequently enter cells probably by endocytosis. Condensation at a lower molar ratio, as displayed by Tat-A_4V_{48}, may have been due to a greater positive charge of the arginine

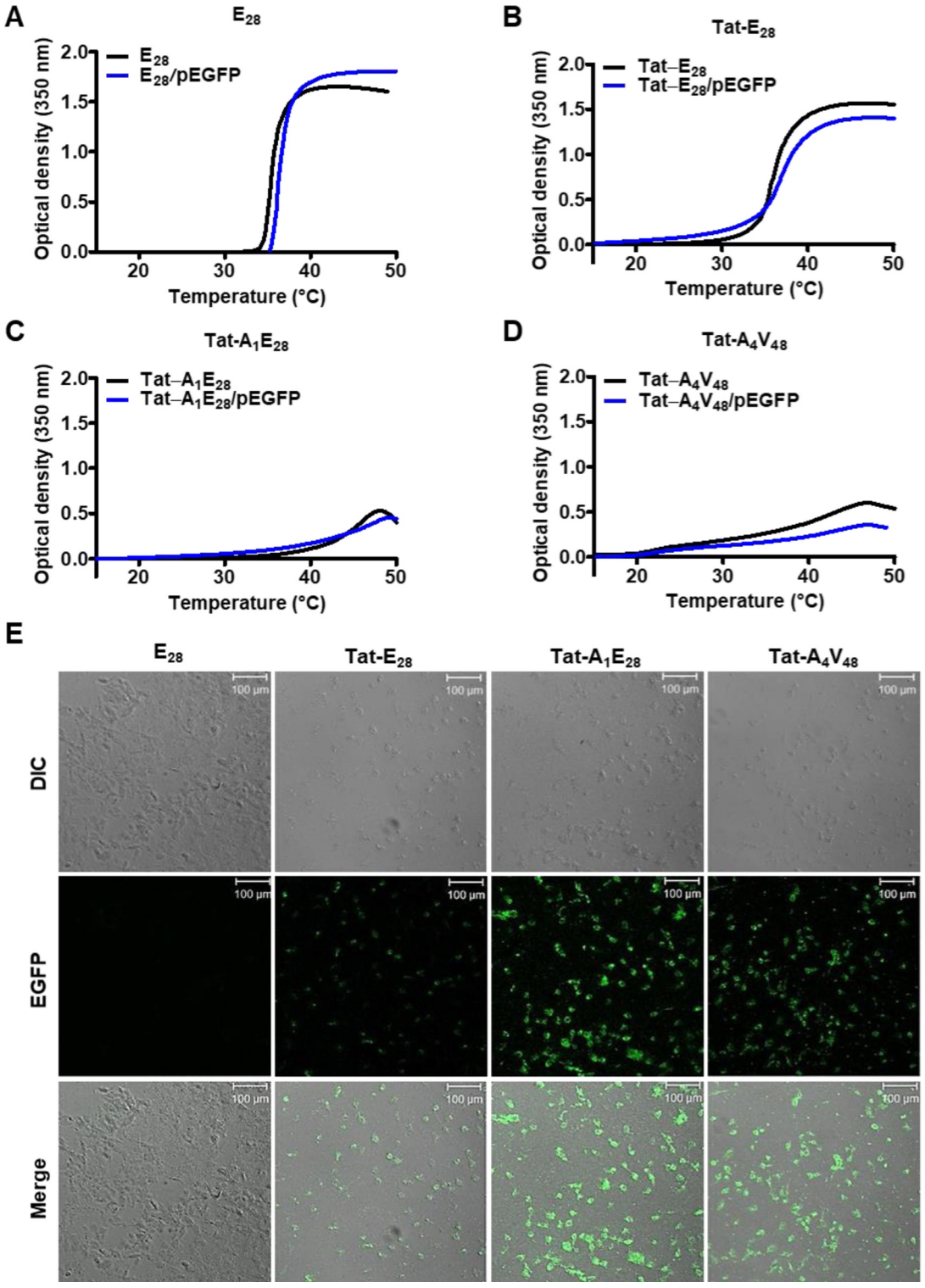

Fig. 2. Thermal characterization of ELPs/pEGFP complexes and analysis of the transfection efficiencies. (A-D) Turbidity profiles of ELPs were determined by observing the optical density (O.D.) at 350 nm while increasing temperature at 1°C/min. The thermal responsiveness of ELPs/pEGFP complexes (Blue) were monitored compared with those of ELP variants at different temperatures. (E) MDA MB231 cells was incubated with ELPs/pEGFP complexes for 6 h at 37 °C and EGFP expression were confirmed by fluorescence microscopy 48 h post-transfection. Scale bar, 100 μm.

residue in Tat and AP-1. E_{28} was not found to condense with nucleic acid, indicating that ELP does not interact with nucleic acid but rather provides thermal responsive self-assembly, shields the DNA molecules, and increases the stability. The designed ELPs variant such as Tat-E_{28}, Tat-A_1E_{28} and Tat-A_4V_{48} protected pEGFP from digestion by DNase I more effectively. The stability of ELPs/pEGFP complexes against DNase I degradation is important for DNA with an intact assembly to advance entry into the nucleus.

The retention of phase transition properties of ELP after condensation with genetic materials are of great importance for effective gene

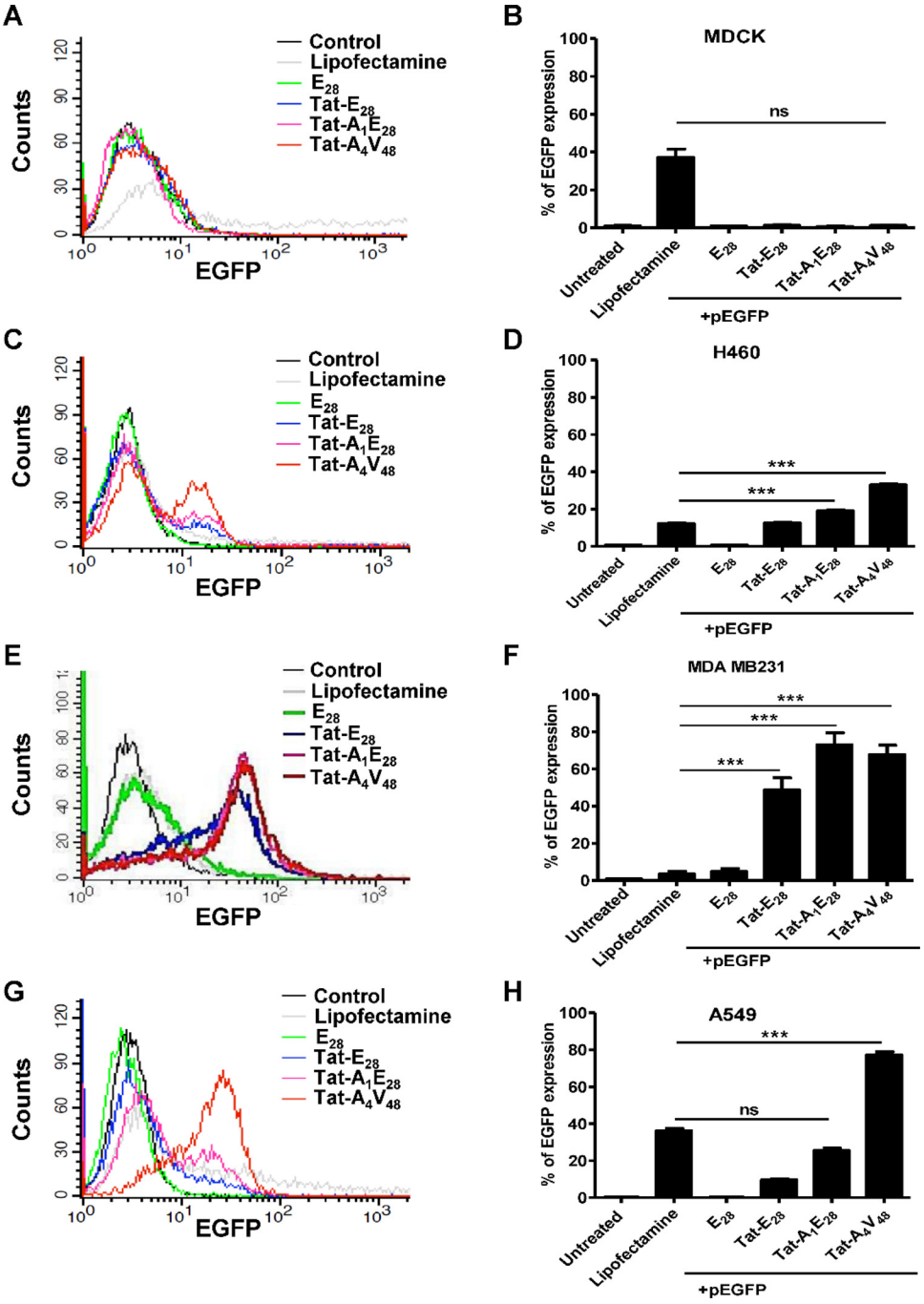

Fig. 3. Transfection efficiencies of ELPs/pEGFP complexes in different cancer cells. Percentages of EGFP expressing in MDCK (A, B), H460 (C, D), MDA MB231 (E, F) and A549 (G, H) cells were analysed in comparison with controls by flow cytomery after 48 h post-transfection (n = 6). Graphical bars (on right) represent the percentage of EGFP expressed cells as mean ±SD of data obtained from six separate experiments performed in triplicate. ***P<0.0001, one-way ANOVA; n = 6.

delivery at therapeutic sites. The slight reduction in Tt clearly indicated an increased hydrophobic effect on complex formation. The positive charges on the ELPs might neutralize the negative charges on pEGFP, thereby remaining in a highly hydrophobic state, which in turn resulted in the depression of Tt [47]. Parallel DLS analysis showed that particle size increased after condensation with pEGFP, which strongly indicates the formation of stable nanocomplexes, and this was confirmed by TEM images. After complexing Tat-A_1E_{28} or Tat-A_4V_{48} with pEGFP molecules, zeta potentials decreased and increased slightly. It was stated that a more positive zeta potentials are advantageous for nanocomplex to increase interactions with cell membranes and entry into cells [48,49]. Thus, the negative zeta potential of Tat-E_{28}/pEGFP might result in low transfection efficiency.

In vitro gene expression analysis of EGFP protein revealed that the higher efficiencies of Tat-A_1E_{28} and Tat-A_4V_{48} transfections than that of Tat-E_{28} into MDA MB231 cells were due to improved cellular uptake. This demonstrated the presence of AP1 peptide resulted in higher EGFP gene expression. In addition, a higher density of positive charges and larger sizes of Tat-A_4V_{48} might increase the cellular membrane association, sedimentation of complexes and gene release. On the other hand, Tat- E_{28} and E_{28} had minimal EGFP gene expression, which evidently showed that Tat peptide had the slightest effect on cellular uptake. In comparison, Lipo 2000 achieved only a 3.3% transfection efficiency in MDA MB231 cells, while it had a 36.2% transfection efficiency in A459 cells. Intriguingly, Lipo 2000 seems to be non-type-specific, whereas Tat-A_1E_{28} and Tat-A_4V_{48} transfections were mediated by IL-4Rs.

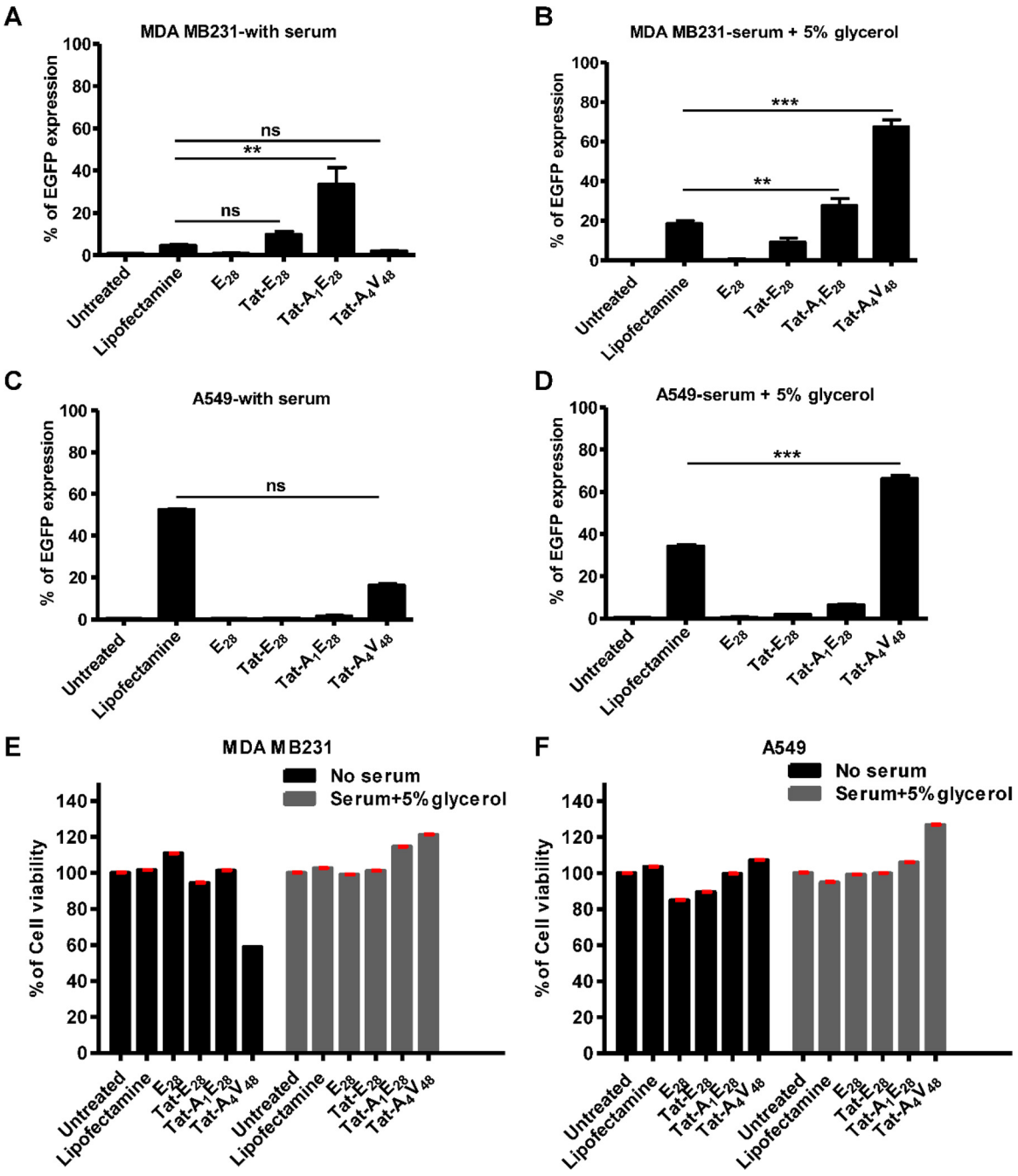

Fig. 4. Evaluation of transfection efficiencies of ELPs/pEGFP complex in different condition. MDA MB231 cells were incubated with ELPs/pEGFP complexes in absence (A) and presence (B) of 5% glycerol under serum condition for 6 h at 37° C. The influence of serum on transfection efficiencies of ELPs/pEGFP complexes was assessed by flow cytometry after 48 h post-transfection. Graphical bars represent the percent of EGFP expressed cells as mean ±SD of data obtained from six separate experiments performed in triplicate. ***P<0.0001, **P<0.001, one-way ANOVA; n = 6. (C-D) Similarly A459 cells were incubated with ELPs/pEGFP complexes in the absence or presence of 5% glycerol under seum conditions and EGFP expression was confirmed after 48 h. (E-F) The percentage of cell viability of both the cells were estimated 48 h post-transfection using CCK-8 kit. Graphical bars (on right) represent the percentage of EGFP expressed cells as mean ±SD of data obtained from six separate experiments performed in triplicate (n = 3).

The serum-tolerance ability of cationic polymers is a vital characteristic for in vivo applications. There is a decrease in Tat-A_4V_{48} transfection when serum is present in MDA MB231 and A549 cells. With 5% glycerol, the efficiency of the transfection system was maintained, despite the presence of serum. It was anticipated that primary amines presence on the Tat-A_4V_{48} polymer surface can easily be associated with serum proteins, which may be a reason for their lower transfection activity under serum conditions. So, further protection of an amine group with glycerol prevents aggregation with serum protein and increased stability of the nanocomplex, resulting in restoring the transfection activity [50]. It was stated that glycerol prevents protein aggregation by inhibiting protein unfolding via interactions with hydrophobic surface residues which in turn stabilizes the aggregation-prone intermediates. Thus, stabilization of the complexes gave the propensity of Tat-A_4V_{48} polymer to retain its transfection activity and exhibit higher transfection activity under serum conditions.

Furthermore, cell viability assays after ELPs/pEGFP complexes transfection produced no evidence of cytotoxicity. Tat-A_4V_{48}/pEGFP com-

plexes treated MDA MB231 cells in the absence of serum showed a decrease in the percentage of cell viability. But when serum was added, cell function was improved and cytotoxicity was reduced. Therefore, these studies suggest Tat-A_4V_{48} displays superior tumor-specific transfection efficacy, serum-tolerance, and low cytotoxicity in various tumor cell lines, making it a safer vehicle for gene transfection.

5. Conclusions

Gene delivery using ELP-based vectors is a promising approach in terms of safety, low cost, and ease of manufacture. The major limitations inherited in other polymers such as cytotoxicity and relatively poor delivery efficiency in the presence of serum can be overcome easily with ELPs. Our data suggest that through multidomain ELP polymer it is possible to achieve cell-specific targeting as a means of facilitating plasmid DNA delivery through receptor-ligand interactions. ELP polymers containing Tat, and AP1 showed considerable potential as a gene delivery system, which increased the versatility for various biomedical applications. It was evidenced that ELP vectors can interact with plasmid DNA and self-assemble to form nanocomplex that were stable under physiological conditions. This system was found to deliver plasmids harboring the EGFP gene selectively and effectively to tumor cells, and enhanced expression of the gene of interest. Thus, we concluded that our designed ELP system fulfills the crucial requirement for efficient delivery vehicle such as (1) successfully condensed with DNA and form stable complexes, which facilitates their cellular uptake and unpacking of the complexes in the cytoplasmic compartment (2) to impart stability to the complexes in the biological environment (3) IL-4R binding ligand enhanced target ability to impart a more efficient cellular uptake. With nanoparticle-DNA complexes gaining successful applications, our designed targeted polymer can be used to deliver functional DNA to target cells. Various tumor models have also been used to conduct studies with nanoparticles to deliver DNA for antitumor treatments. We suggest that the described ELP-based systems offer a promising strategy for gene therapy applications that specifically target tumor cells expressing IL-4R at high levels.

Declaration of Competing Interest

The authors declare no conflict of interest.

Acknowledgments

This study was supported by National Research Foundation of Korea (NRF), Korea government (MSIT), Grant (No. 2021R1A5A2021614).

Supplementary materials

Supplementary material associated with this article can be found, in the online version, at doi:10.1016/j.bbiosy.2022.100050.

References

[1] Mukherjee S, Thrasher AJ. Gene therapy for PIDs: progress, pitfalls and prospects. Gene 2013;525:174–81. doi:10.1016/j.gene.2013.03.098.
[2] Yla-Herttuala S, Alitalo K. Gene transfer as a tool to induce therapeutic vascular growth. Nat Med 2003;9:694–701. doi:10.1038/nm0603-694.
[3] Cooper MJ. Noninfectious gene transfer and expression systems for cancer gene therapy. Semin Oncol 1996;23:172–87.
[4] Bunnell BA, Morgan RA. Gene therapy for infectious diseases. Clin Microbiol Rev 1998;11:42–56. doi:10.1128/CMR.11.1.42.
[5] de Fougerolles A, Vornlocher HP, Maraganore J, Lieberman J. Interfering with disease: a progress report on siRNA-based therapeutics. Nat Rev Drug Discov 2007;6:443–53. doi:10.1038/nrd2310.
[6] Juliano R, Alam MR, Dixit V, Kang H. Mechanisms and strategies for effective delivery of antisense and siRNA oligonucleotides. Nucl Acids Res 2008;36:4158–71. doi:10.1093/nar/gkn342.
[7] van den Boorn JG, Schlee M, Coch C, Hartmann G. SiRNA delivery with exosome nanoparticles. Nat Biotechnol 2011;29:325–6. doi:10.1038/nbt.1830.
[8] Zhou J, Shum KT, Burnett JC, Rossi JJ. Nanoparticle-based delivery of RNAi therapeutics: progress and challenges. Pharmaceuticals (Basel) 2013;6:85–107. doi:10.3390/ph6010085.
[9] Al-Dosari MS, Gao X. Nonviral gene delivery: principle, limitations, and recent progress. AAPS J 2009;11:671–81. doi:10.1208/s12248-009-9143-y.
[10] Konstan MW, Davis PB, Wagener JS, Hilliard KA, Stern RC, Milgram LJ, Kowalczyk T H, SL Hyatt, Fink TL, Gedeon CR, et al. Compacted DNA nanoparticles administered to the nasal mucosa of cystic fibrosis subjects are safe and demonstrate partial to complete cystic fibrosis transmembrane regulator reconstitution. Hum Gene Ther 2004;15:1255–69. doi:10.1089/hum.2004.15.1255.
[11] Ramamoorth M, Narvekar A. Non viral vectors in gene therapy- an overview. J Clin Diagn Res 2015;9:GE01–6. doi:10.7860/JCDR/2015/10443.5394.
[12] Fischer D, Bieber T, Li Y, Elsasser HP, Kissel T. A novel non-viral vector for DNA delivery based on low molecular weight, branched polyethylenimine: effect of molecular weight on transfection efficiency and cytotoxicity. Pharm Res 1999;16:1273–9. doi:10.1023/a:1014861900478.
[13] Lundberg P, El-Andaloussi S, Sutlu T, Johansson H, Langel U. Delivery of short interfering RNA using endosomolytic cell-penetrating peptides. FASEB J 2007;21:2664–71. doi:10.1096/fj.06-6502com.
[14] Vives E. Present and future of cell-penetrating peptide mediated delivery systems: "is the trojan horse too wild to go only to troy? J Control Release 2005;109:77–85. doi:10.1016/j.jconrel.2005.09.032.
[15] Derossi D, Joliot AH, Chassaing G, Prochiantz A. The third helix of the antennapedia homeodomain translocates through biological membranes. J Biol Chem 1994;269:10444–50.
[16] Vives E, Brodin P, Lebleu B. A truncated HIV-1 tat protein basic domain rapidly translocates through the plasma membrane and accumulates in the cell nucleus. J Biol Chem 1997;272:16010–17. doi:10.1074/jbc.272.25.16010.
[17] Sadler K, Eom KD, Yang JL, Dimitrova Y, Tam JP. Translocating proline-rich peptides from the antimicrobial peptide bactenecin 7. Biochemistry 2002;41:14150–7. doi:10.1021/bi026661l.
[18] Hong CA, Nam YS. Functional nanostructures for effective delivery of small interfering RNA therapeutics. Theranostics 2014;4:1211–32. doi:10.7150/thno.8491.
[19] Son S, Namgung R, Kim J, Singha K, Kim WJ. Bioreducible polymers for gene silencing and delivery. Acc Chem Res 2012;45:1100–12. doi:10.1021/ar200248u.
[20] Peng Q, Zhong Z, Zhuo R. Disulfide cross-linked polyethylenimines (PEI) prepared via thiolation of low molecular weight PEI as highly efficient gene vectors. Bioconjug Chem 2008;19:499–506. doi:10.1021/bc7003236.
[21] Faltus T, Yuan J, Zimmer B, Kramer A, Loibl S, Kaufmann M, Strebhardt K. Silencing of the HER2/neu gene by siRNA inhibits proliferation and induces apoptosis in HER2/neu-overexpressing breast cancer cells. Neoplasia 2004;6:786–95. doi:10.1593/neo.04313.
[22] Chen T-H H, Bae Y, Furgeson DY. Intelligent biosynthetic nanobiomaterials (IBNs) for hyperthermic gene delivery. Pharm Res 2008;25:683–91. doi:10.1007/s11095-007-9382-5.
[23] Monfort DA, Koria P. Recombinant elastin-based nanoparticles for targeted gene therapy. Gene Therapy 2017;24:610–20. doi:10.1038/gt.2017.54.
[24] Dash BC, Mahor S, Carroll O, Mathew A, Wang W, Woodhouse KA, et al. Tunable elastin-like polypeptide hollow sphere as a high payload and controlled delivery gene depot. J Control Release 2011;152:382–92. doi:10.1016/j.jconrel.2011.03.006.
[25] MacEwan SR, Chilkoti A. Elastin-like polypeptides: biomedical applications of tunable biopolymers. Biopolymers 2010;94:60–77. doi:10.1002/bip.21327.
[26] Meyer DE, Chilkoti A. Purification of recombinant proteins by fusion with thermally-responsive polypeptides. Nat Biotechnol 1999;17:1112–15. doi:10.1038/15100.
[27] Meyer DE, Chilkoti A. Genetically encoded synthesis of protein-based polymers with precisely specified molecular weight and sequence by recursive directional ligation: examples from the elastin-like polypeptide system. Biomacromolecules 2002;3:357–67. doi:10.1021/bm015630n.
[28] Javier AF, Santos M, Fernández-Colino A, Pinedo G, Girotti A. Recent contributions of elastin-like recombinamers to biomedicine and nanotechnology. Curr Top Med Chem 2014;14:819–36. doi:10.2174/1568026614666140118223412.
[29] Garcia-Arevalo C, Bermejo-Martin JF, Rico L, Iglesias V, Martin L, Rodriguez-Cabello JC, et al. Immunomodulatory nanoparticles from elastin-like recombinamers: single-molecules for tuberculosis vaccine development. Mol Pharmaceut 2013;10:586–97. doi:10.1021/mp300325v.
[30] de Torre IG, Wolf F, Santos M, Rongen L, Alonso M, Jockenhoevel S, Rodríguez-Cabello JC, Mela P. Elastin-like recombinamer-covered stents: towards a fully biocompatible and non-thrombogenic device for cardiovascular diseases. Acta Biomaterialia 2015;12:146–55. doi:10.1016/j.actbio.2014.10.029.
[31] McDaniel JR, MacEwan SR, Dewhirst M, Chilkoti A. Doxorubicin-conjugated chimeric polypeptide nanoparticles that respond to mild hyperthermia. J Control Release 2012;159:362–7. doi:10.1016/j.jconrel.2012.02.030.
[32] Rodríguez-Cabello JC, Piña MJ, Ibáñez-Fonseca A, Fernández-Colino A, Arias FJ. Nanotechnological approaches to therapeutic delivery using elastin-like recombinamers. Bioconjugate Chem 2015;26:1252–65. doi:10.1021/acs.bioconjchem.5b00183.
[33] Rincon A, Molina-Martinez I, de Las Heras B, Alonso M, Bailez C, Rodríguez-Cabello J, Herrero-Vanrell R. Biocompatibility of elastin-like polymer poly (VPAVG) microparticles: in vitro and in vivo studies. J Biomed Mater Res A 2006;78:343–51. doi:10.1002/jbm.a.30702.
[34] Trabbic-Carlson K, Meyer D, Liu La, Piervincenzi R, Nath N, LaBean T, Chilkoti A. Effect of protein fusion on the transition temperature of an environmentally responsive elastin-like polypeptide: a role for surface hydrophobicity? Protein Eng Des Sel 2004; 17: 57-66. doi: 10.1093/protein/gzh006
[35] Christensen T, Hassouneh W, Trabbic-Carlson K, Chilkoti A. Predicting transition temperatures of elastin-like polypeptide fusion proteins. Biomacromolecules 2013;14:1514–19. doi:10.1021/bm400167h.
[36] Walker L, Perkins E, Kratz F, Raucher D. Cell penetrating peptides fused to a thermally targeted biopolymer drug carrier improve the delivery and antitumor effi-

cacy of an acid-sensitive doxorubicin derivative. Int. J. Pharm 2012;436:825–32. doi:10.1016/j.ijpharm.2012.07.043.
[37] Bidwell GL III, D Raucher. Cell penetrating elastin-like polypeptides for therapeutic peptide delivery. Adv Drug Deliv Rev 2010;62:1486–96. doi:10.1016/j.addr.2010.05.003.
[38] Pina MJ, Alex SM, Arias FJ, Santos M, Rodriguez-Cabello JC, Ramesan RM, et al. Elastin-like recombinamers with acquired functionalities for gene-delivery applications. J Biomed Mater Res A 2015;103:3166–78. doi:10.1002/jbm.a.35455.
[39] Hy Hong, Lee HY, Kwak W, Yoo J, Na MH, So IS, Kwon TH, Park HS, Huh S, Oh GT. Phage display selection of peptides that home to atherosclerotic plaques: IL-4 receptor as a candidate target in atherosclerosis. J Cell Mol Med 2008;12:2003–14. doi:10.1111/j.1582-4934.2008.00189.x.
[40] Park K, Hong H-Y, Moon HJ, Lee B-H, Kim I-S, Kwon IC, et al. A new atherosclerotic lesion probe based on hydrophobically modified chitosan nanoparticles functionalized by the atherosclerotic plaque targeted peptides. J Control Release 2008;128:217–23. doi:10.1016/j.jconrel.2008.03.019.
[41] Obiri NI, Hillman GG, Haas GP, Sud S, Puri RK. Expression of high affinity interleukin-4 receptors on human renal cell carcinoma cells and inhibition of tumor cell growth in vitro by interleukin-4. J Clin Investig 1993;91:88–93. doi:10.1172/JCI116205.
[42] Obiri N, Siegel J, Varricchio F, Puri R. Expression of High-affinity IL-4 receptors on human melanoma, ovarian and breast carcinoma cells. Clin Exp Immunol 1994;95:148–55. doi:10.1111/j.1365-2249.1994.tb06029.x.
[43] Husain SR, Gill P, Kreitman RJ, Pastan I, Puri RK. Interleukin-4 receptor expression on AIDS-associated Kaposi's Sarcoma cells and their targeting by a chimeric protein comprised of circularly permuted interleukin-4 and pseudomonas exotoxin. Mol Med 1997;3:327–38. doi:10.1007/BF03401811.
[44] Kawakami K, Leland P, Puri RK. Structure, function, and targeting of interleukin 4 receptors on human head and neck cancer cells. Cancer Res 2000;60:2981–7.
[45] Yi A, Sim D, Lee Y-J, Sarangthem V, Park R-W. Development of elastin-like polypeptide for targeted specific gene delivery in vivo. J Nanobiotechnol 2020;18:1–14. doi:10.1186/s12951-020-0574-z.
[46] Zeng X, Pan S, Li J, Wang C, Wen Y, Wu H, Wang C, Wu C, Feng M. A novel dendrimer based on poly (L-glutamic acid) derivatives as an efficient and biocompatible gene delivery vector. Nanotechnology 2011;22:375102. doi:10.1088/0957-4484/22/37/375102.
[47] Urry DW. Free energy transduction in polypeptides and proteins based on inverse temperature transitions. Prog Biophys Mol Biol 1992;57:23–57. doi:10.1016/0079-6107(92)90003-o.
[48] Blau S, Jubeh TT, Haupt SM, Rubinstein A. Drug targeting by surface cationization. Crit Rev Ther Drug Carrier Syst 2000;17:425–65. doi:10.1615/CritRevTherDrugCarrierSyst.v17.i5.10.
[49] Cao D, Qin L, Huang H, Feng M, Pan S, Chen J. Transfection activity and the mechanism of pDNA-complexes based on the hybrid of low-generation PAMAM and branched PEI-1.8 k. Mol BioSyst 2013;9:3175–86. doi:10.1039/c3mb70261h.
[50] Vagenende V, Yap MG, Trout BL. Mechanisms of protein stabilization and prevention of protein aggregation by glycerol. Biochemistry 2009;48:11084–96. doi:10.1021/bi900649t.